Escola de Primavera de Transição e Turbulência
Blumenau 2022

ABCM
13th Spring School on Transition and Turbulence
September 19th-23rd, 2022, Blumenau, SC, Brazil

EPTT-2022-XXXX
Simulation Of Premixed Propane Turbulent Flow Using A Multicomponent All-Mach Solver.

Vinícius Hagemeyer Chiumento
Alex José Elias
Freddy Portillo Morales
João Marcelo Vedovotto
Federal University of Uberlândia - Av. João Naves de Ávila, 2121 - Santa Mônica, Uberlândia - MG, 38408-100
e-mails:
vini.hagemeyer@gmail.com
alex.elias@ufu.br
freddyalejandropm@ufps.edu.co
vedovotto@ufu.br

Abstract. *A multi-component All-Mach solver is developed at the Laboratorio de Mecânica dos Fluidos (MFLab) in the Multi-Physics Simulator (MFSim) environment. The code uses a finite volume scheme featuring total variation diminishing (TVD) discretization methods, immersed boundary method (IBM), and SIMPLE family algorithm, such as Semi-Implicit Method for Pressure-Linked Equations (SIMPLE), Semi-Implicit Method for Pressure Linked Equations-Consistent (SIMPLEC) and Pressure-Implicit with Splitting of Operators (PISO). The code is used to study a non-reactive Volvo burner case with a bluff-body. The case assessed in the present work was studied experimentally in the Volvo Flygmotor AB program, the experimental results of the non-reactive case are compared with the results obtained by MFSim. The simulations are performed using a propane gas mixture, with their properties being evaluated through the CANTERA software. RANS and Large Eddy Simulation (LES) and the All-Mach PISO algorithm. The results agree with the experimental data.*

Keywords: *Turbulent flow, Immersed Boundary Method, All-Mach.*

1. INTRODUCTION

A numerical simulation is an important tool in many engineering cases, such as aerodynamics, turbo-machinery, propulsion systems, and others. On turbulent reactive flows, the mixing process is very important affecting the final result, especially when is used a combustion model based on the mixing process . The purpose of this work is to simulate compressible flows with high or low Mach Numbers conferring the accuracy of turbulence methodology on inert flows.

The validation is performed with a simulation of a propane flow in a duct with a bluff-body is performed. The conditions are similar to the Volvo burner that was studied experimentally in the Volvo Flygmotor AB program. The simulation is performed at low Mach Number considering chemical species transport, and fluid properties are obtained considering pressure, temperature and composition of the mixture inside a volume. The simulations were carried out using the MFSim software, under development at the Fluid Mechanics Laboratory - MFLab, at the Federal University of Uberlândia.

Several numerical methods are implemented in the MFSim platform to simulate multiphase turbulent reactive flows with complex geometries and physical phenomena. The code uses block-structured adaptive mesh refinement, with an All-Mach solver and immersed boundary method. The properties of the fluid are obtained using the library Cantera in the function of Temperature, pressure, and mass fraction of chemical species. The code developed can be extended to include combustion models based on mixing process like eddy break-up model (EBM), Conserved Scalar model (CSM) and Bray-Moss-Libby (BML).

2. NUMERICAL MODEL

The set of equations solved in the current modeling study are Navier-Stokes equations, as well as energy and mass balance. Equation 1 are the three-dimensional Navier-Stokes equations for compressible flows where u is the fluid velocity, P is the pressure, μ is the viscosity of fluid and ρ is the density. The term f_i is the result of direct forcing method

$$\frac{\partial \rho u_i}{\partial t} + \frac{\partial \rho u_i u_j}{\partial x_i} = -\frac{\partial P}{\partial x_i} + \frac{\partial}{\partial x_i}\left[\mu\left(\frac{\partial u_i}{\partial x_j} + \frac{\partial u_j}{\partial x_i}\right) - \frac{2}{3}\mu\left(\frac{\partial u_k}{\partial x_k}\right)\right] + f_i \tag{1}$$

The energy transport is modeled by eq. 2 where T is the temperature, C_p is the Specific heat capacity at constant pressure and k is the thermal conductive capacity. The 2 equation contains the term Φ, which is viscous energy dissipation

and describes the conversion of mechanical energy into heat. A detailed description of Φ is shown in eq. 3.

$$\frac{\partial \rho c_p T}{\partial t} + \frac{\partial \rho c_p T u_i}{\partial x_i} = \frac{\partial}{\partial x_i}\left(k\frac{\partial T}{\partial x_i}\right) + \Phi + \frac{\partial P}{\partial t} + u_i\frac{\partial P}{\partial x_i} \tag{2}$$

$$\Phi = 2\mu\left(S_{ij}S_{ij} - \frac{1}{3}S_{kk}^2\right) \tag{3}$$

$$S_{ij} = \frac{1}{2}\left(\frac{\partial \bar{u_i}}{\partial x_j} + \frac{\partial \bar{u_j}}{\partial x_i}\right) \tag{4}$$

The transport of chemical species are modeled by eq.5 where Y_k is the mass fraction of a chemical specie k, D_k is the diffusion coefficient, and $\dot{\omega}_k$ is the source therm modeling the production and consumption of a chemical specie.

$$\frac{\partial}{\partial t}(\rho Y_k) + \frac{\partial}{\partial x_i}(\rho u_i Y_k) = \frac{\partial}{\partial x_i}\left[\left(\rho D_k + \frac{\mu_t}{Sc_t}\right)\frac{\partial Y_k}{\partial x_i}\right] + \dot{\omega}_k \tag{5}$$

Another relevant equation is the mass balance equation presented in eq. 6 The equation of state (eq. 7) is used to obtain the density field as a function of pressure, temperature, and gas constant (R).

$$\frac{\partial \rho}{\partial t} + \frac{\partial \rho u_i}{\partial x_i} = 0 \tag{6}$$

$$\rho = \frac{p}{RT} \tag{7}$$

The LES method utilised are described by Vreman (2004), and indicated for cases with near-wall regions because the dissipation is relatively small in this regions. This model usually results in better results than Smagorinsky model, especially in internal flows.

2.1 PRESSURE VELOCITY COUPLING

A modified version of the PISO algorithm is used to couple pressure and velocity. The algorithm can solve two or more pressure correction equations. Equation 8 is the pressure correction equation derived from eq. 5. In the case of compressible flows, there are extra terns in equations than the traditional incompressible PISO algorithm.

$$\frac{\partial \frac{P'}{RT}}{\Delta t} + \frac{\partial u_i^*(\frac{P'}{RT})}{\partial x_i} + \frac{\partial}{\partial x_i}\left(-\frac{\rho^*}{Ap}\frac{\partial P'}{\partial x_i}\right) = \frac{\partial(\rho^* - \rho^0)}{\Delta t} + \frac{\partial u_i^*(\rho^*)}{\partial x_i} \tag{8}$$

In Low-Mach flows, the first term on the right-hand side will be very small, as the first and second term on the left-hand side. If these terms are disregarded, the original equation for pressure correction for the incompressible PISO algorithm will be recovered. The compressible PISO algorithm can solve flows with a low Mach Number or High Mach number as well as a flow with a region at Low Mach Numbers and another at High Mach Numbers resulting in an All-Mach solver (Moukalled and Darwish, 2000). The second pressure correction is presented in eq. 9.

$$\frac{\partial \rho^{***}}{\partial t} + \frac{\partial}{\partial x_i}\left(\rho^{**}u_i^{**} + \rho^{**}\sum A(u_i^{**} - u_i^*)/A + \rho^{**}D(P'') + C_P P'' u_i^{**}\right) = 0 \tag{9}$$

The corrected pressure is obtained by eq. 10. A density correction is calculated by eq 11. The superscript denotes an initial estimated value and the superscript $'$ denote a correction value. Also the superscripts and $''$ represent the value estimate by the previous correction and the second correction. At least, the first correction of velocity is shown in eq. 12.

$$P = P^* + P' \tag{10}$$

$$\rho = \rho^* + \rho' = \rho^* + \frac{P'}{RT} \tag{11}$$

$$u_i = u_i^* + u_i' = u_i^* - \frac{1}{A_p^u}\left(\frac{\Delta p'}{\Delta X}\right)_p \tag{12}$$

The complete PISO algorithm is described below:

1. Solve energy equation and mass fractions equation.

Case	Non-reacting	Reacting
Re	48 000	48 000
U_{bulk}	16,6 m/s	17,3 m/s
ϕ	0,0	0,65
T_{in}	288 k	288 k

Table 1. Initial conditions of Volvo burner.

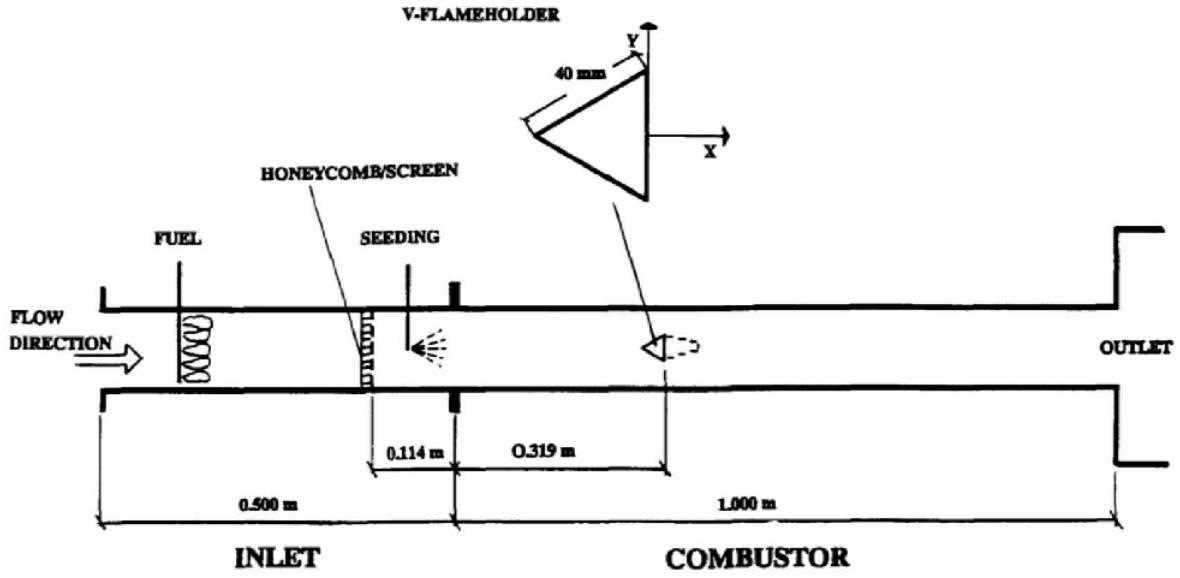

Figure 1. Sketch of the test section used in the experiment, adapted from (Sjunnesson *et al.*, 1992).

2. Update properties using Cantera.
3. Solve momentum equation to obtain predictions of u^*.
4. Solve pressure correction equation 8.
5. Correct P, u and ρ.
6. Solve the second pressure equation 9.
7. Correct P, u and ρ.
8. Repeat step 6-7 until convergence or reach maximum number of inner-loop PISO iterations.
9. Step 1-8 are repeated until the solutions are sufficiently converged.
10. Compute direct forcing for momentum.
11. Advance in time and return to step 1 until reach the final time of simulation.

Advection terms are discretized using TVD Quick, for time integration SBDF (semi-implicit backward differencing) is used. Typically, the PISO inner-loop is limited to 3 iterations. The time step is defined by CLF criteria (Courant–Friedrichs–Lewy), when $CFL = 0.2$.

3. CASE DESCRIPTION AND NUMERICAL SETUP

The Volvo burner features a bluff-body stabilized premixed flame, this case was studied experimentally by Sjunnesson *et al.* (1992) and numerically by Elias *et al.* (2018), Fureby and Moller (1995), and Sankaran and Gallagher (2017). A few simulations will be performed using this configuration and the numerical methods described above. At the input the axial velocity has a fully developed turbulent profile, the gas composition is $Y_{c_3h_8} = 0.04007047$,$Y_{O_2} = 0.2236633$,$Y_{n_2} = 0.73626623$. The operating conditions are described in tab. 1. The computational domain is in agreement with the experimental case illustrated in fig 1. The same measurements are utilized in the computational experiment.

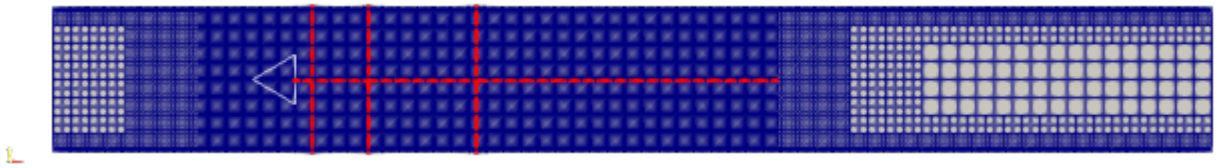

Figure 2. Computational grid, the red dot line represent position of probes.

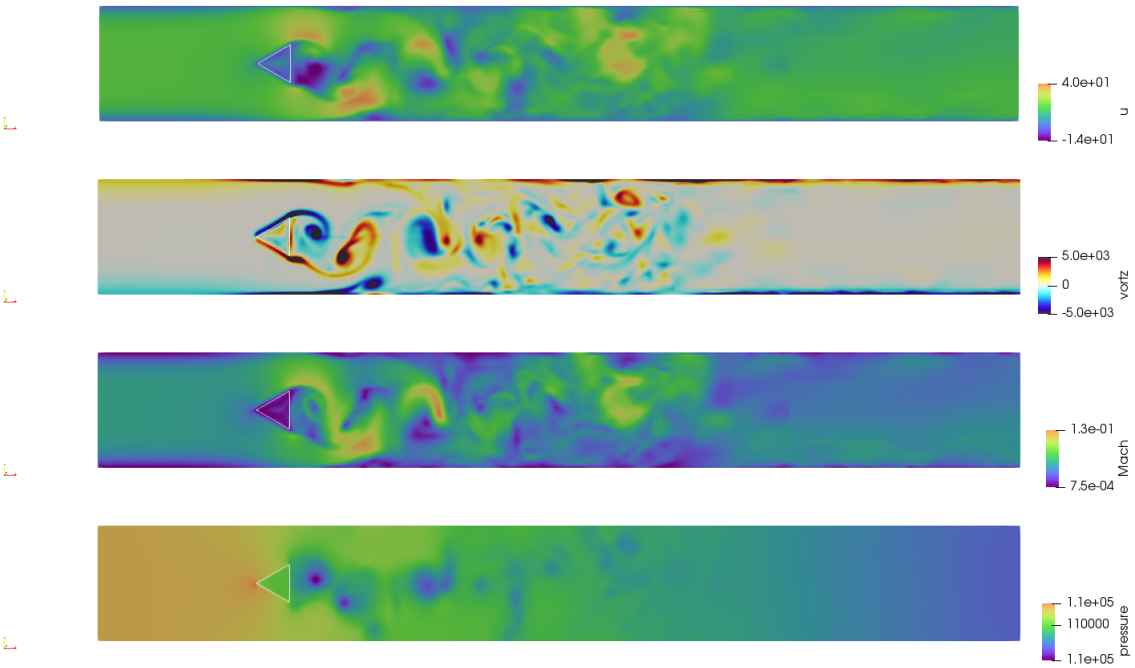

Figure 3. From top to button, instantaneous contours of component u of velocity, vorticity in the z direction, Mach Number, and pressure inside the burner. The write solid line represents the immersed boundary.

An inlet boundary condition is considered at the west face of the domain, in the east face is defined as an outlet boundary condition. The north and south faces are wall boundary conditions, and for the faces in the z direction a symmetry condition is defined. The immersed boundary condition is a non-slip wall.

The computational grid and the lines where the probes are placed are shown in fig. 2. The probes get data each time step for statistical analysis, the position of the probes is defined according to the red dots in fig. 2. Although the code can use adaptive mesh refinement, in this particular case the mesh is constant to avoid a fine mesh in the output reducing the computational cost at the end of the simulation. The mesh contains 667.648 volumes with the smallest volume of $\Delta x = \Delta y = 0,001875m$. The simulations are performed using LES.

4. RESULTS

Figure 3 shows instantaneous contours of component u of velocity, vorticity in z direction, Mach Number, and pressure inside the burner. It is possible to see the formation of coherent structures after the buff body, at the end of the burner the vortices are suppressed in the coarse mesh region. The maximum local Mach Number is around 0.13, indicating a little influence of compressible effects on the flow.

Figures 4 and 5 show the profiles for mean axial velocity and RMS axial velocity in three different positions. The results show a good agreement with the experiment for the mean axial velocity. As expected when using LES the RMS axial velocity differs from the experiment, that is more accentuated near to flameholder ($x = 0.215$). The same comportment is reported by Elias *et al.* (2018).

The comportment of transverse velocity is similar to axial velocity. Figure 6 and 7 shows the mean transverse velocity and the RMS transverse velocity. The Reynolds stress profile is plotted in figure 8. Figure 9 shows the mean axial velocity, anisotropy, and fluctuation level downstream the flameholder. The iso-contour of Q-criterium is presented in fig. 10, the contours are colored by instantaneous axial velocity.

To test the capabilities of the solver, a transonic case was proposed based on the Volvo burner. Figure 11 shows

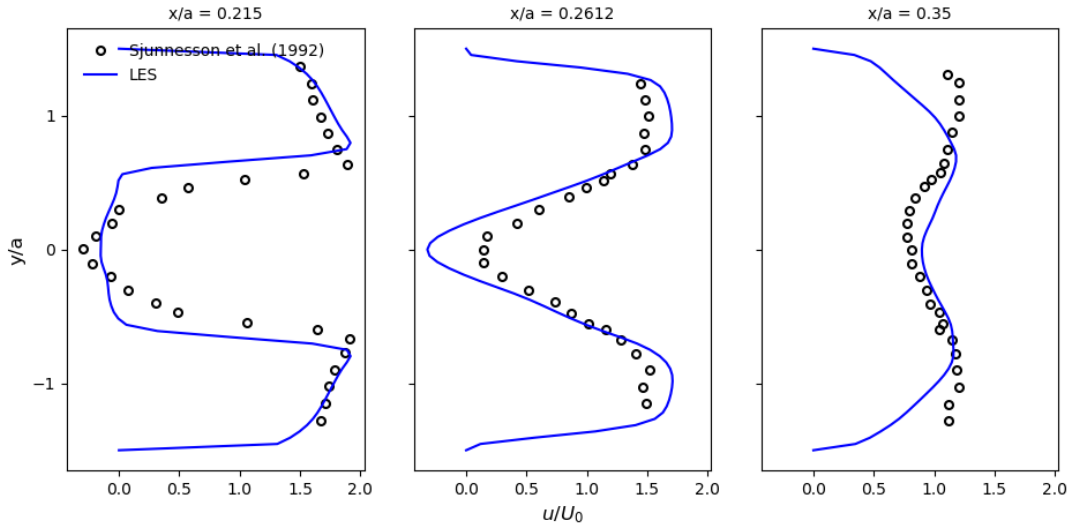

Figure 4. Normalized mean axial velocity profile downstream the flameholder, experimental results indicated by circles, and LES results represented by a solid blue line.

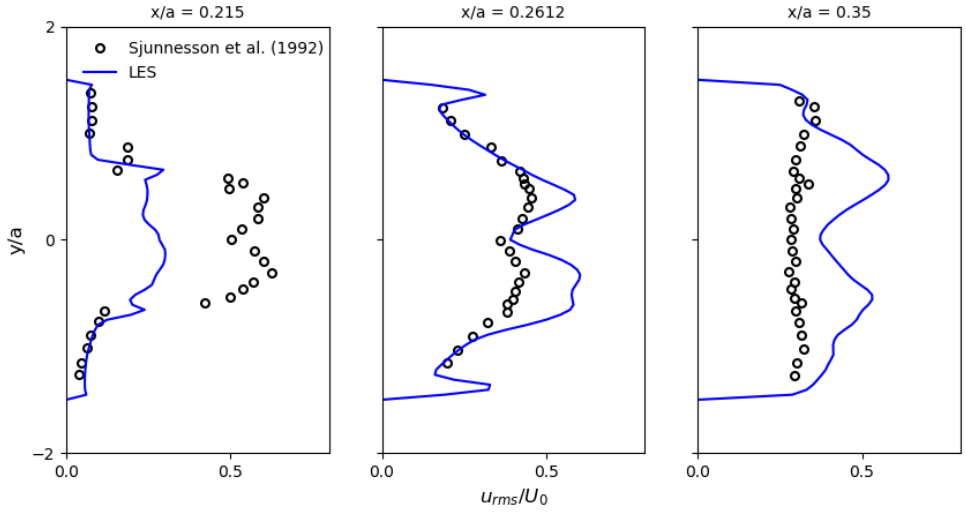

Figure 5. Normalized RMS axial velocity profile downstream the flameholder, experimental results indicated by circles, and LES results represented by a solid blue line.

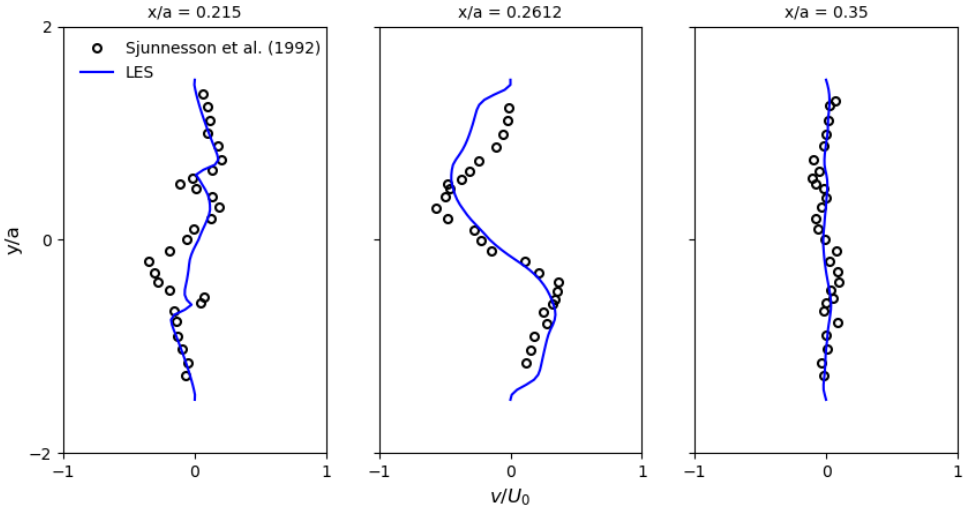

Figure 6. Normalized mean transverse velocity profile downstream the flameholder, experimental results indicated by circles, and LES results represented by a solid blue line.

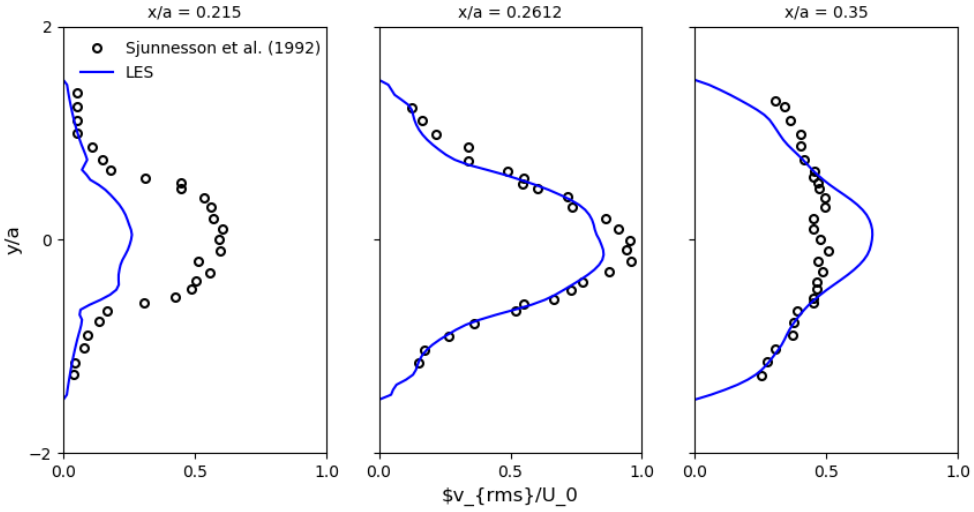

Figure 7. Normalized RMS transverse velocity profile downstream the flameholder, experimental results indicated by circles, and LES results represented by a solid blue line.

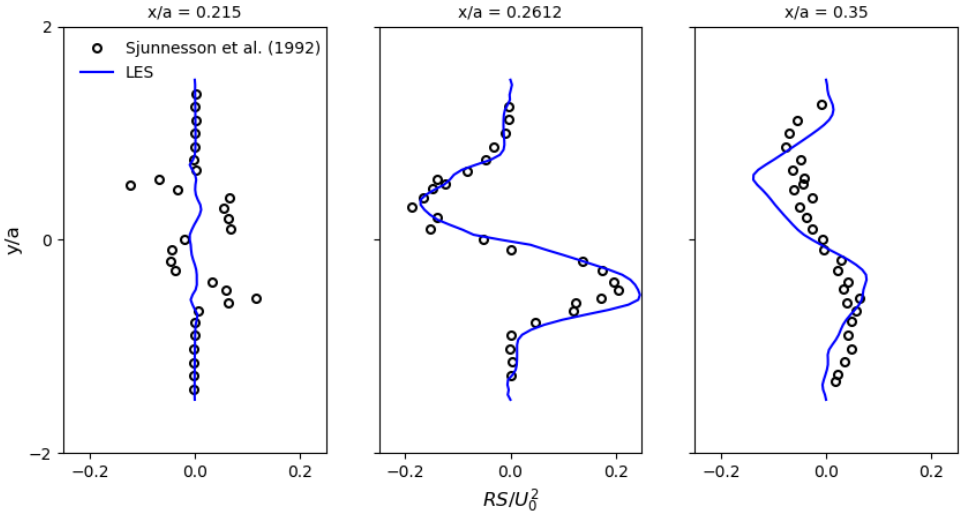

Figure 8. Normalized mean Reynolds stress profiles downstream the flameholder, experimental results indicated by circles and LES results represented by solid blue line.

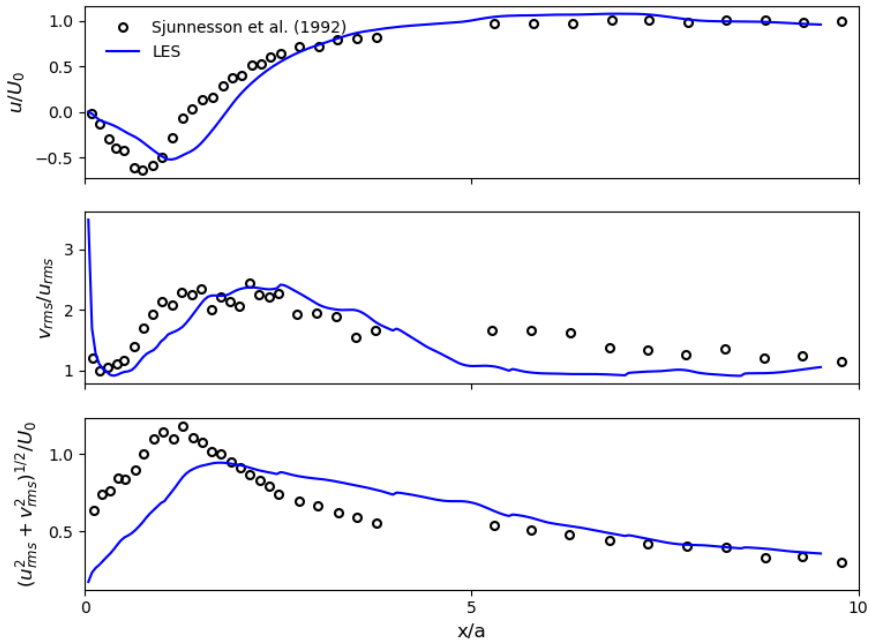

Figure 9. Centerline profiles from top to button mean axial velocity, anisotropy, and fluctuation level downstream the flameholder. Experimental results indicated by circles and LES results represented by solid blue line.

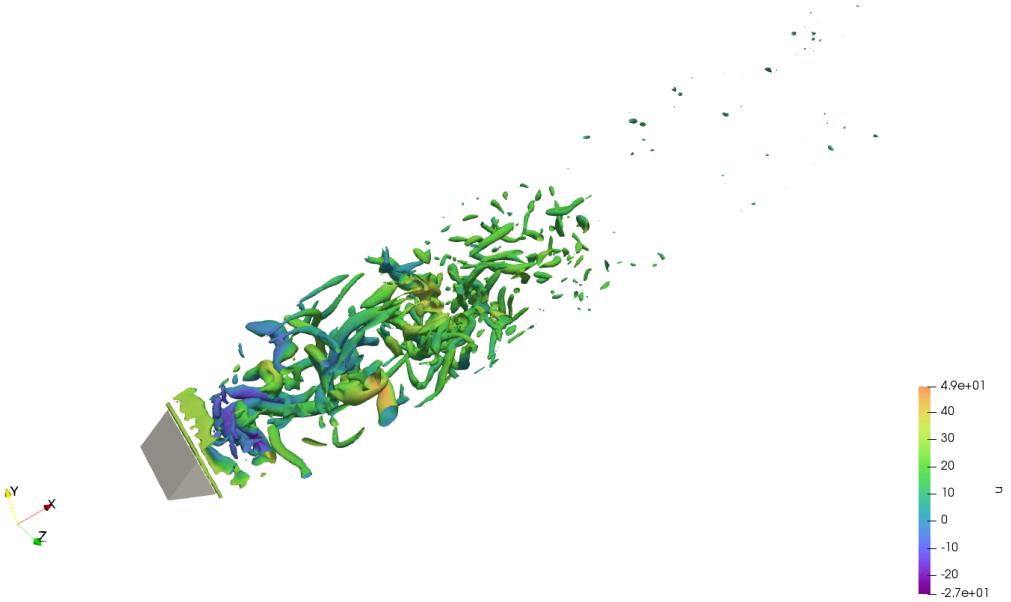

Figure 10. Iso contour for Q-criterion colored by instantaneous axial velocity.

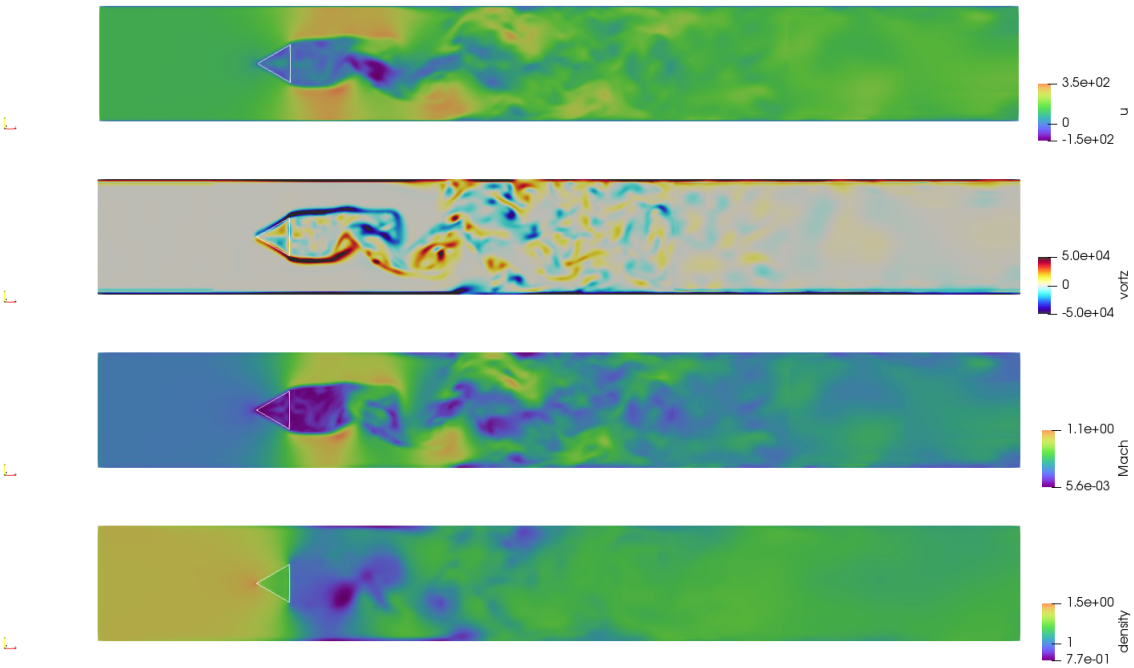

Figure 11. From top to button, instantaneous contours of component u of velocity, vorticity in the z-direction, Mach Number, and density inside the burner. The white solid line represents the immersed boundary.

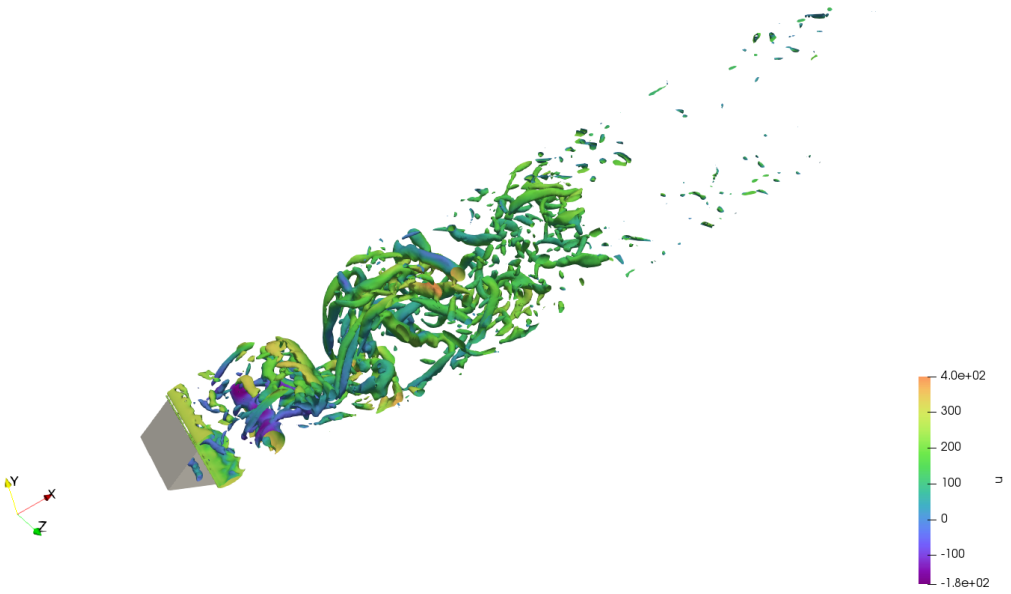

Figure 12. Caption

instantaneous contours of component u of velocity, vorticity in the z-direction, Mach Number, and density inside the burner for a transonic case. This case is similar to the previous one with high inlet velocity ($u = 148m/s$) resulting in $M = 0.43$. The results are only qualitative, some regions show $M > 1$, indicating a supersônic region. a shock wave almost is formed at the end of flameholder. In the recirculation zone after the flameholder is very small close to zero. The code demonstrates to be able to handle a variation of Mach Number inside the computational domain. Figure **??** show the contours of Q-criterion colored by instantaneous axial velocity.

5. CONCLUSIONS AND FUTURE WORK

The simulation of a low Mach flow inside a bluff-body burner agrees with the experimental results. The code was able to resolve compressible flows with the transport of chemical species and variable fluid properties. Also, the solver can be used for transonic and supersonic flows. The LES methodology utilized works very well in the case of study. The next step is to extend the capabilities code, such as for solving reactive flows that can be used in a wide variety of applications in the industry environment.

6. ACKNOWLEDGEMENTS

The authors would like to thank Foz do Chapecó, Baesa, Enercan and Ceran for technical and financial support, through the Research and Development project PD-02949-3007/2022 – "Solução integrada para o diagnóstico de defeitos, análise dinâmica e monitoramento contínuo de unidades geradoras francis" with resources from ANEEL's RD program. The authors also would like to thank Petrobras, CNPq, FAPEMIG, and CAPES (INCT-EIE) for the financial support of the present contribution.

7. CONCLUSIONS

8. REFERENCES

Elias, A.J. *et al.*, 2018. "Modelagem híbrida urans-les para escoamentos turbulentos".

Fureby, C. and Moller, S.I., 1995. "Large eddy simulation of reacting flows applied to bluff body stabilized flames". *AIAA journal*, Vol. 33, No. 12, pp. 2339–2347.

Moukalled, F. and Darwish, M., 2000. "A unified formulation of the segregated class of algorithms for fluid flow at all speeds". *NUMERICAL HEAT TRANSFER PART B FUNDAMENTALS*, Vol. 37, No. 1, pp. 103–139.

Sankaran, V. and Gallagher, T., 2017. "Grid convergence in les of bluff body stabilized flames". In *55th AIAA Aerospace Sciences Meeting*. p. 1791.

Sjunnesson, A., Henrikson, P. and Lofstrom, C., 1992. "Cars measurements and visualization of reacting flows in a bluff body stabilized flame". In *28th Joint Propulsion Conference and Exhibit*. p. 3650.

Vreman, A., 2004. "An eddy-viscosity subgrid-scale model for turbulent shear flow: Algebraic theory and applications".

Physics of fluids, Vol. 16, No. 10, pp. 3670–3681.

9. RESPONSIBILITY NOTICE

The authors are the only responsible for the printed material included in this paper.